

**Supporting Information for:**

**A Cobalt-Nitrosyl Complex with a Hindered  
Hydrotris(pyrazolyl)borate Coligand: Detailed Electronic Structure,  
and Reactivity towards Dioxygen**

**Kiyoshi Fujisawa,<sup>\*,a</sup> Shoko Soma,<sup>a</sup> Haruka Kurihara,<sup>a</sup> Hai T. Dong,<sup>b</sup>  
Max Bilodeau,<sup>b</sup> and Nicolai Lehnert<sup>\*,b</sup>**

<sup>a</sup> Department of Chemistry, Ibaraki University, Mito 310-8512, Japan

<sup>b</sup> Department of Chemistry and Department of Biophysics, University of Michigan, 930 N. University  
Avenue, Ann Arbor, Michigan, 48109, United States

<b>Table S1</b>	X-ray crystallographic data for [Co(NO)(L3)], [Co( $\eta^2$ -O <sub>2</sub> N)(L3)], and [Co( $\eta^2$ -O <sub>2</sub> NO)(L3)]	S2
<b>Figures S1-S2</b>	IR spectra of [Co(NO) <sub>2</sub> (tmeda)](BPh <sub>4</sub> ) and [Co(NO)(L3)]	S3
<b>Figure S3</b>	Far-IR spectra of [Co(NO)(L3)]	S4
<b>Figure S4</b>	IR spectra of [Co( $\eta^2$ -O <sub>2</sub> N)(L3)] and [Co( $\eta^2$ -O <sub>2</sub> NO)(L3)]	S4
<b>Figure S5</b>	UV-Vis and DR spectra of [Co(NO)(L3)]	S5
<b>Figure S6</b>	UV-Vis spectra of [Co( $\eta^2$ -O <sub>2</sub> N)(L3)] and [Co( $\eta^2$ -O <sub>2</sub> NO)(L3)]	S5
<b>Figure S7</b>	<sup>1</sup> H-NMR spectrum of [Co(NO)(L3)]	S6
<b>Figure S8</b>	<sup>1</sup> H-NMR spectrum of [Co( $\eta^2$ -O <sub>2</sub> N)(L3)]	S6
<b>Figure S9</b>	<sup>1</sup> H-NMR spectrum of [Co( $\eta^2$ -O <sub>2</sub> NO)(L3)]	S6
<b>Figure S10</b>	IR spectral changes by the reaction of O <sub>2</sub> in the solution state	S7
<b>Figure S11</b>	UV-Vis spectral changes by the reaction of O <sub>2</sub> in the solution state	S7
<b>Figure S12</b>	UV-Vis spectral comparisons	S8
<b>Figure S13</b>	IR spectral changes by the reaction of O <sub>2</sub> in the solid state	S8
<b>Figure S14</b>	<sup>1</sup> H-NMR spectrum after the reaction of [Co(NO)(L3)] with O <sub>2</sub> in the solution	S9
<b>Figure S15</b>	<sup>1</sup> H-NMR spectrum after the reaction of [Co(NO)(L3)] with O <sub>2</sub> in the solid	S9
<b>Table S2</b>	MO charge distributions for [Co(NO)(L0)] (B3LYP/TZVP)	S10
<b>Tables S3-S4</b>	Coordinates of the fully optimized structure of [Co(NO)(L0)]	S11-S12

**Table S1.** X-ray crystallographic data for [Co(NO)(L3)], [Co( $\eta^2$ -O<sub>2</sub>N)(L3)], and [Co( $\eta^2$ -O<sub>2</sub>NO)(L3)].

	[Co(NO)(L3)]	[Co( $\eta^2$ -O <sub>2</sub> N)(L3)]	[Co( $\eta^2$ -O <sub>2</sub> NO)(L3)]
CCDC deposit num.	1534553	1534554	1534555
Empirical formula	C <sub>30</sub> H <sub>52</sub> BCoN <sub>7</sub> O	C <sub>30</sub> H <sub>52</sub> BCoN <sub>7</sub> O <sub>2</sub>	C <sub>30</sub> H <sub>52</sub> BCoN <sub>7</sub> O <sub>3</sub>
Formula weight	596.53	612.53	628.53
Crystal system	Monoclinic	Monoclinic	Monoclinic
Space group	<i>P</i> <sub>2</sub> <sub>1</sub> / <i>n</i> (No. 14)	<i>P</i> <sub>2</sub> <sub>1</sub> / <i>n</i> (No. 14)	<i>P</i> <sub>2</sub> <sub>1</sub> / <i>m</i> (No. 11)
<i>a</i> /Å	9.5351(9)	9.4573(13)	9.4152(13)
<i>b</i> /Å	17.2416(19)	17.404(2)	17.442(2)
<i>c</i> /Å	20.421(2)	20.336(3)	10.6017(16)
$\beta$ /°	99.585(3)	100.603(3)	106.857(3)
<i>V</i> /Å <sup>3</sup>	3310.4(6)	3290.0(8)	1666.2(4)
<i>Z</i>	4	4	2
<i>D</i> <sub>calc</sub> /gcm <sup>-3</sup>	1.197	1.237	1.253
<i>R</i> (int)	0.0309	0.0289	0.0315
$\mu$ (Mo <i>K</i> $\alpha$ ) /cm <sup>-1</sup>	5.517	5.590	5.558
Reflections collected	53745	53446	27761
Unique reflections	7582	7548	3927
No. of variables	361	370	211
Reflections/para. ratio	21.00	20.40	18.61
<i>R</i> ( <i>I</i> > 2 $\sigma$ ( <i>I</i> ))	0.0431	0.0303	0.0276
<i>R</i> (All reflections)	0.0592	0.0440	0.0311
<i>R</i> <sub>w</sub> (All reflections)	0.1209	0.0752	0.0727
Good. of fit indicator	1.039	1.019	1.054
Max/min peak, /e Å <sup>3</sup>	1.92 / -0.49	0.36 / -0.25	0.40 / -0.34

$$R = \frac{\sum ||Fo| - |Fc||}{\sum |Fo|}; R_w = \left[ \frac{\sum w(Fo^2 - Fc^2)^2}{\sum w(Fo^2)^2} \right]^{1/2}$$

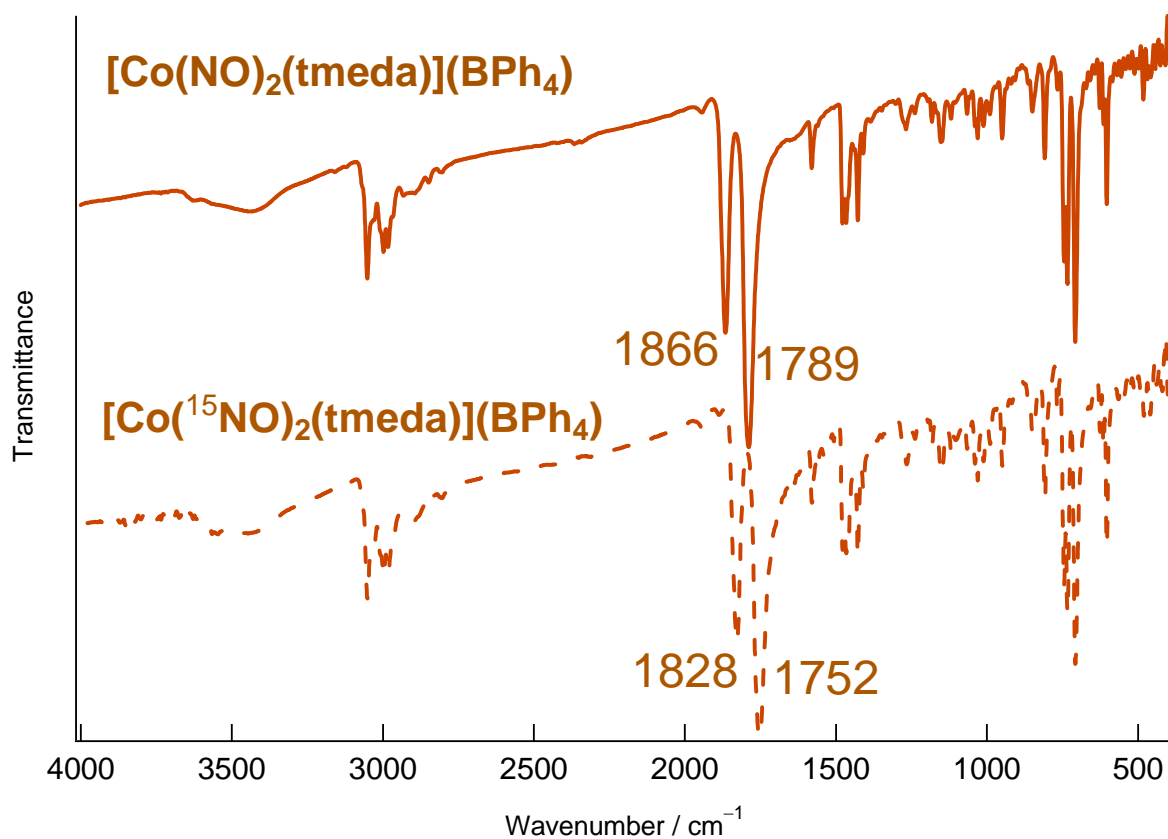


**Figure S1.** IR spectra of  $[\text{Co}(\text{NO})_2(\text{tmeda})](\text{BPh}_4)$  (solid line) and  $[\text{Co}({}^{15}\text{NO})_2(\text{tmeda})](\text{BPh}_4)$  (dotted line).

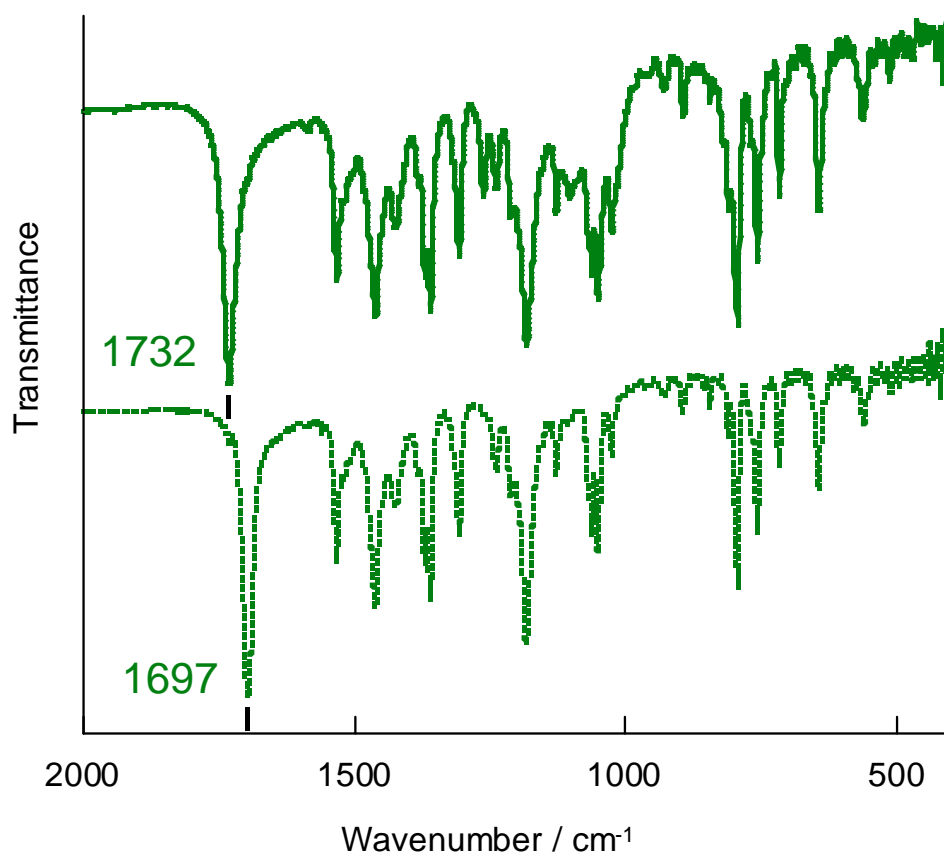


**Figure S2.** IR spectra of  $[\text{Co}(\text{NO})(\text{L3})]$  (solid line) and  $[\text{Co}({}^{15}\text{NO})(\text{L3})]$  (dotted line).

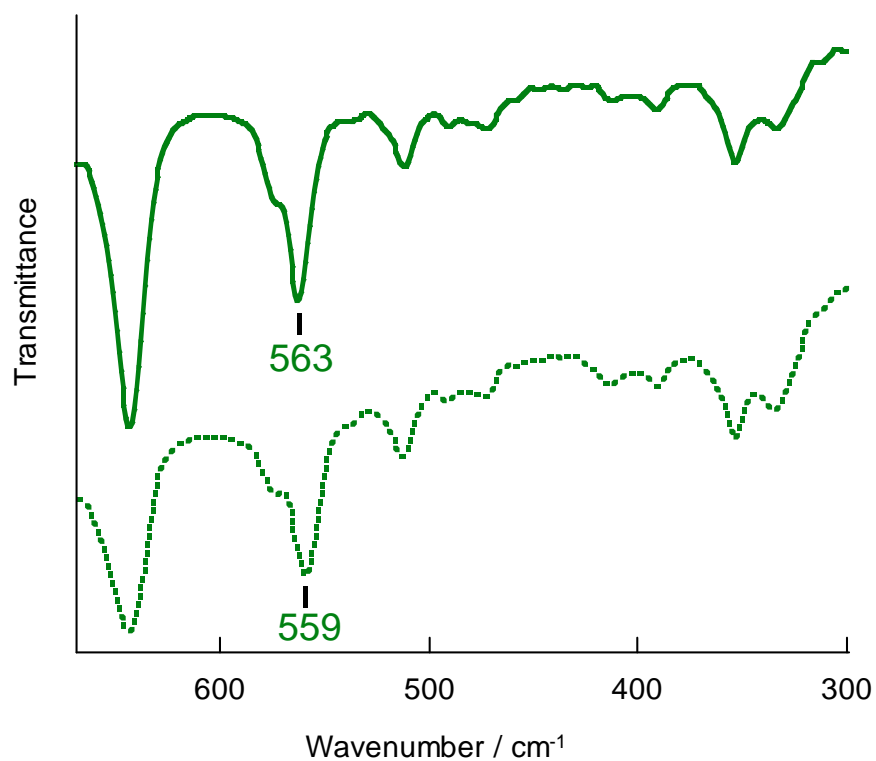


**Figure S3.** Far-IR spectra of  $[\text{Co}(\text{NO})(\text{L3})]$  (solid line) and  $[\text{Co}(\text{}^{15}\text{NO})(\text{L3})]$  (dotted line).

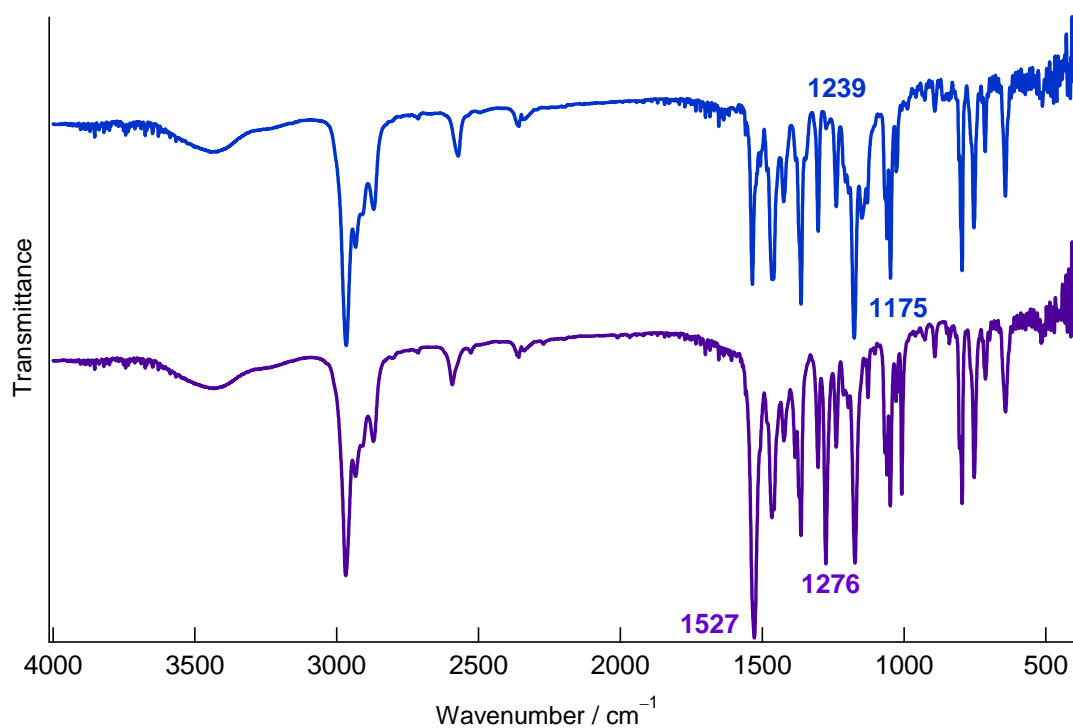


**Figure S4.** IR spectra of  $[\text{Co}(\eta^2\text{-O}_2\text{N})(\text{L3})]$  (top) and  $[\text{Co}(\eta^2\text{-O}_2\text{NO})(\text{L3})]$  (bottom).

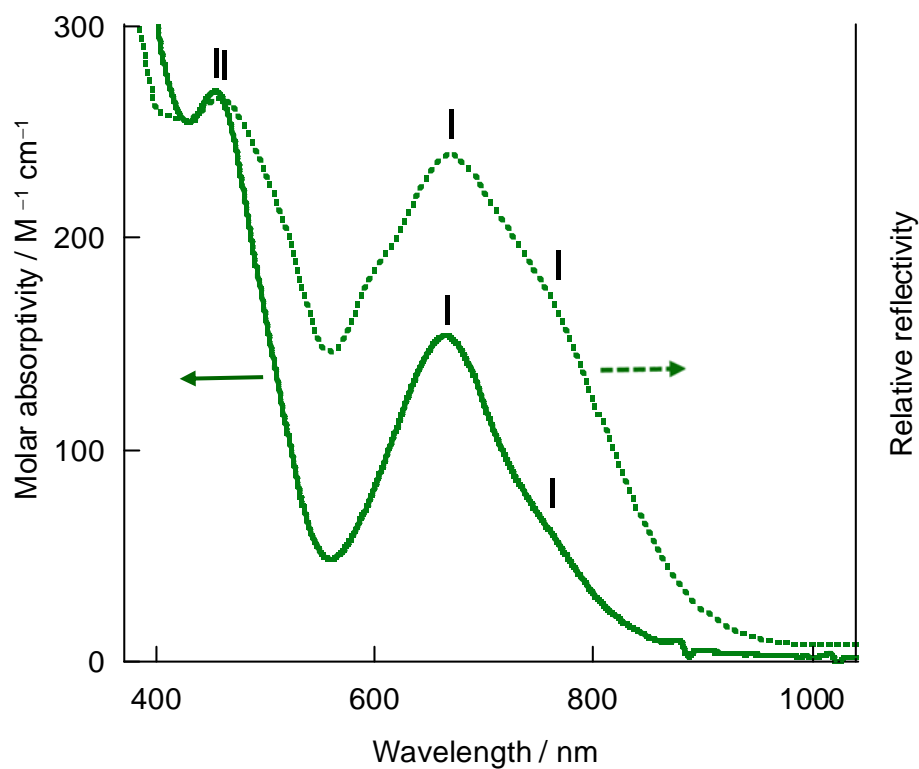


**Figure S5.** UV-Vis (solid line) and diffuse reflectance (DR, dotted line) spectra of  $[\text{Co}(\text{NO})(\text{L3})]$ .

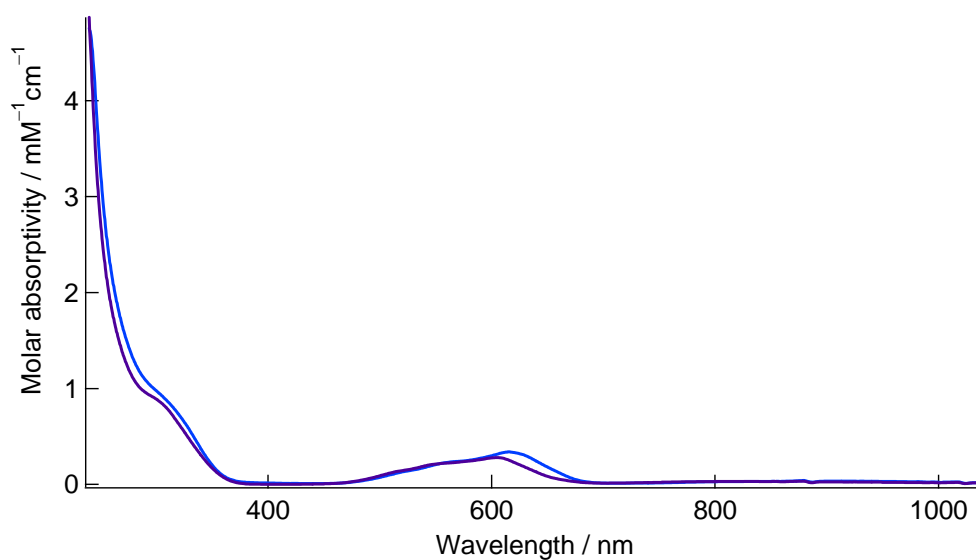


**Figure S6.** UV-Vis spectra of  $[\text{Co}(\eta^2\text{-O}_2\text{N})(\text{L3})]$  (blue) and  $[\text{Co}(\eta^2\text{-O}_2\text{NO})(\text{L3})]$  (purple).

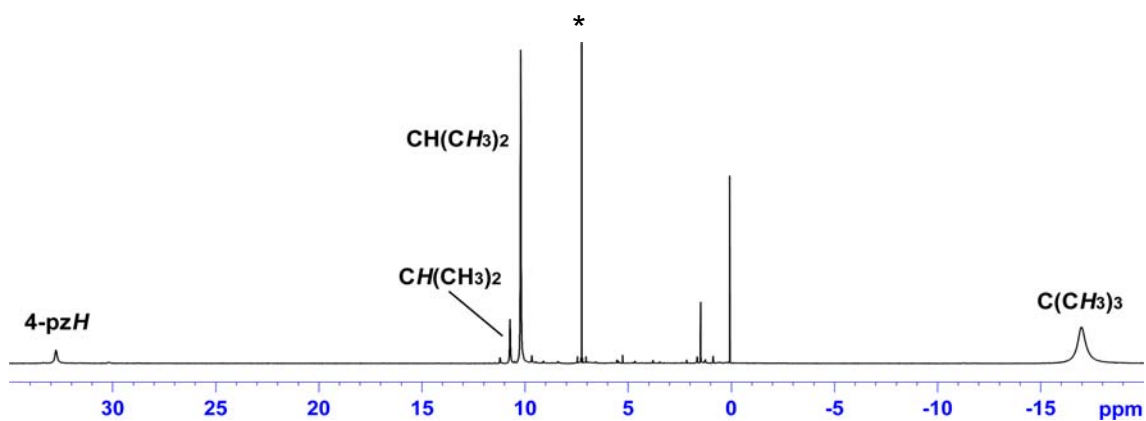


**Figure S7.**  $^1\text{H-NMR}$  spectrum of  $[\text{Co}(\text{NO})(\text{L3})]$  in  $\text{CDCl}_3$  at room temperature (\* marks solvents and TMS peaks).

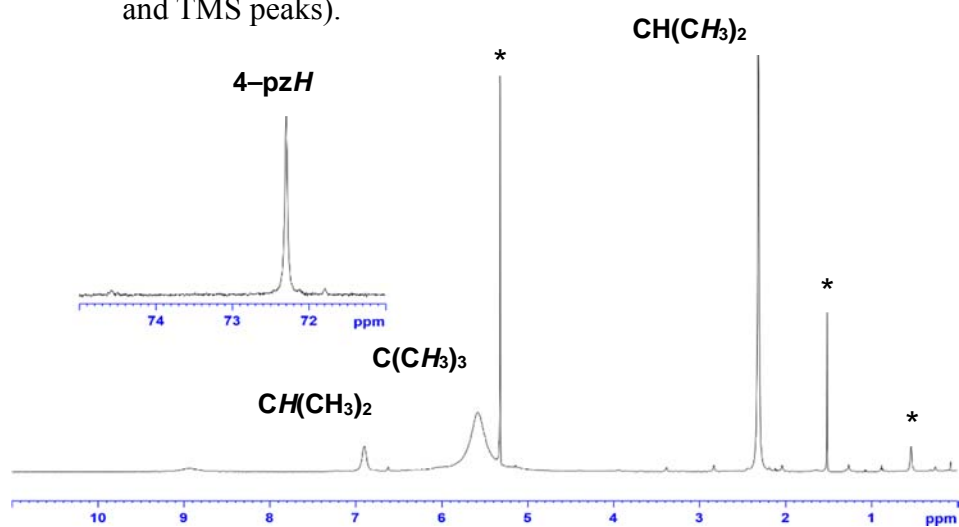


**Figure S8.**  $^1\text{H-NMR}$  spectrum of  $[\text{Co}(\eta^2\text{-O}_2\text{N})(\text{L3})]$  in  $\text{CD}_2\text{Cl}_2$  at room temperature (\* marks solvents and impurities peaks).

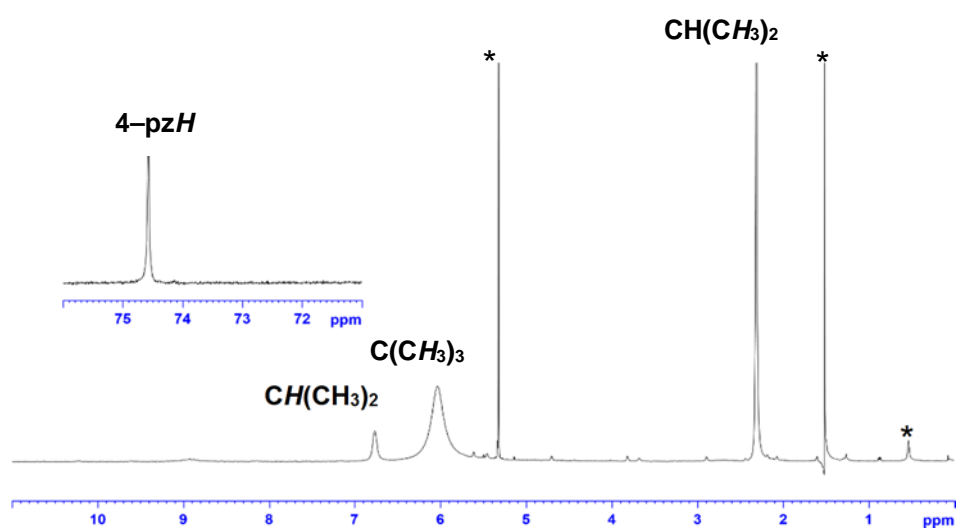


**Figure S9.**  $^1\text{H-NMR}$  spectrum of  $[\text{Co}(\eta^2\text{-O}_2\text{NO})(\text{L3})]$  in  $\text{CD}_2\text{Cl}_2$  at room temperature (\* marks solvents and impurities peaks).

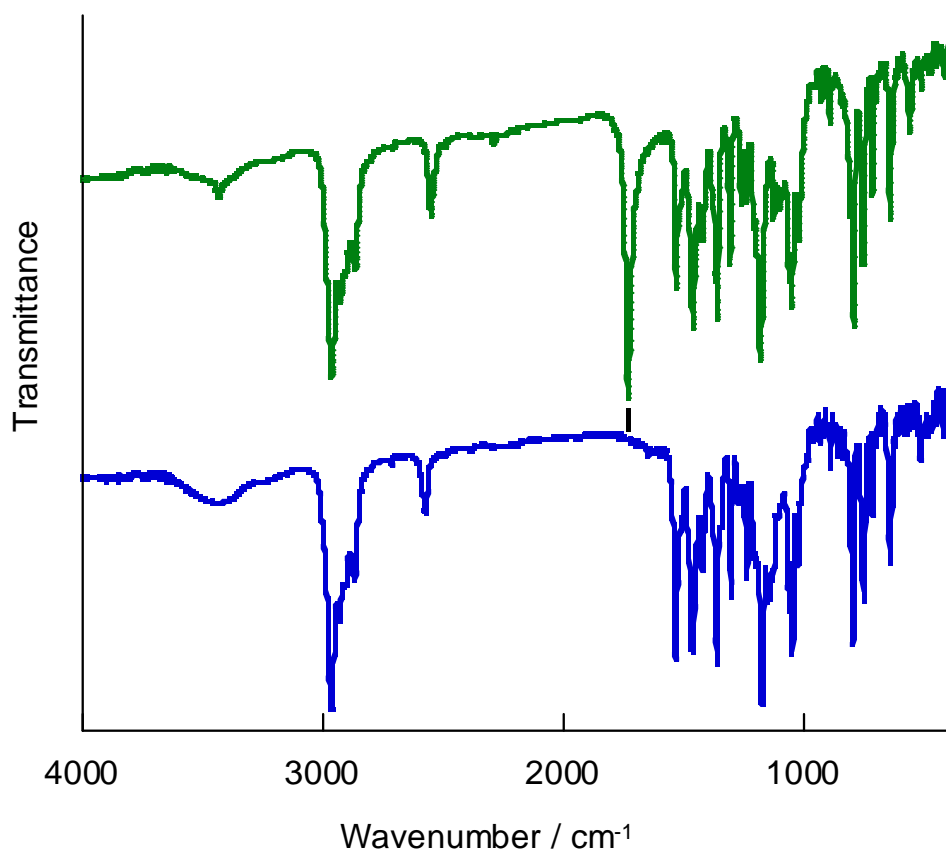


**Figure S10.** IR spectral changes during the O<sub>2</sub> reaction of [Co(NO)(L3)] in solution: before O<sub>2</sub> addition (green) and after the reaction (blue).

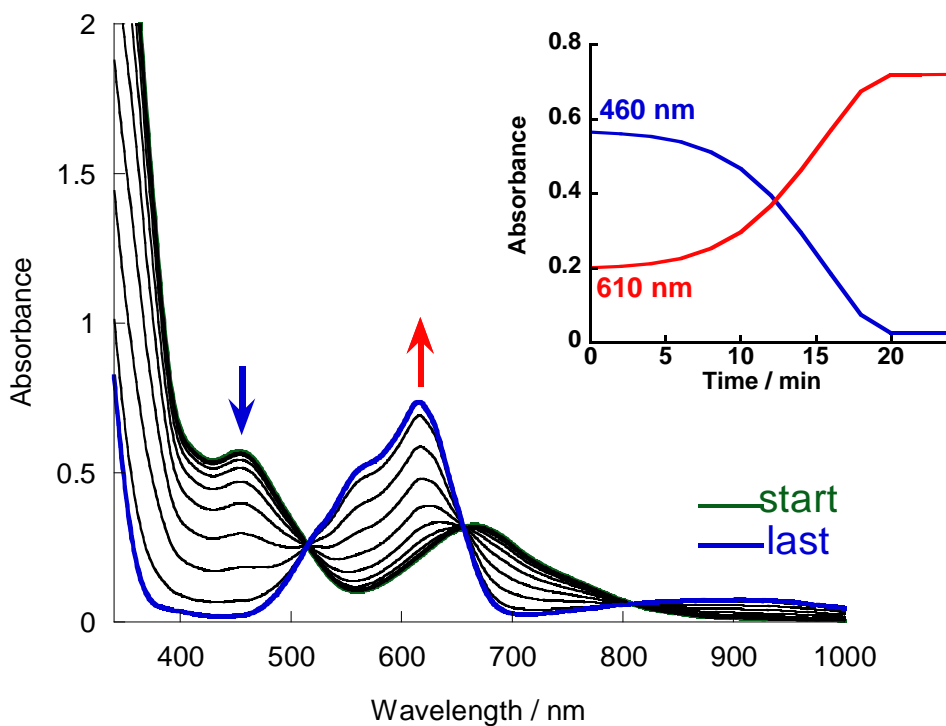


**Figure S11.** UV-Vis spectral changes during the reaction of [Co(NO)(L3)] with O<sub>2</sub> in the solution state (spectra taken every 2 min): before O<sub>2</sub> addition (green) and after the reaction (blue). Inset: time dependent changes at 460 (blue) and 610 nm (red).

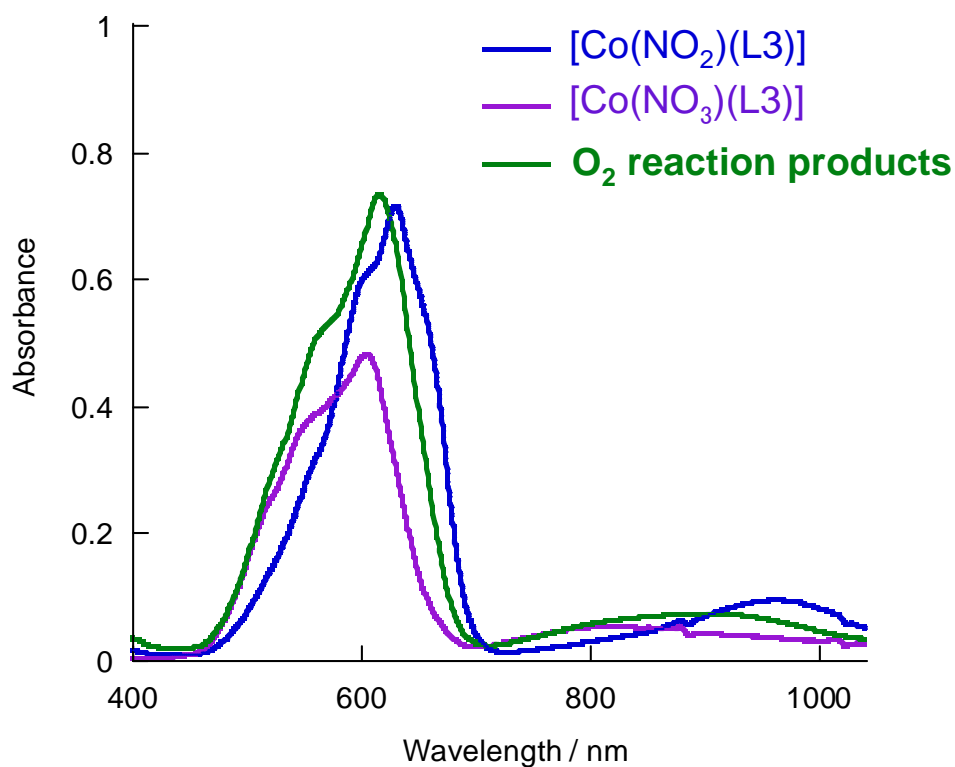


**Figure S12.** UV-Vis spectral comparison between the cobalt(II) complexes  $[\text{Co}(\eta^2\text{-O}_2\text{N})(\text{L3})]$  (blue) and  $[\text{Co}(\eta^2\text{-O}_2\text{NO})(\text{L3})]$  (purple) and the  $\text{O}_2$  reaction products of  $[\text{Co}(\text{NO})(\text{L3})]$  (green; after 20 min reaction time).

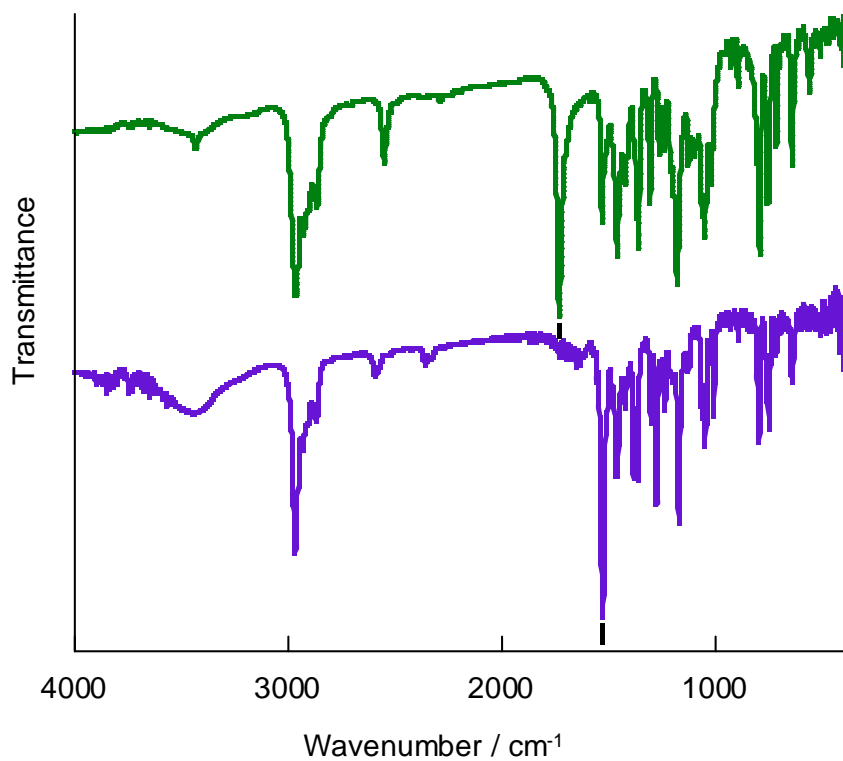


**Figure S13.** IR spectral changes during the  $\text{O}_2$  reaction of  $[\text{Co}(\text{NO})(\text{L3})]$  in the solid state: before  $\text{O}_2$  addition (green) and after the reaction (purple).



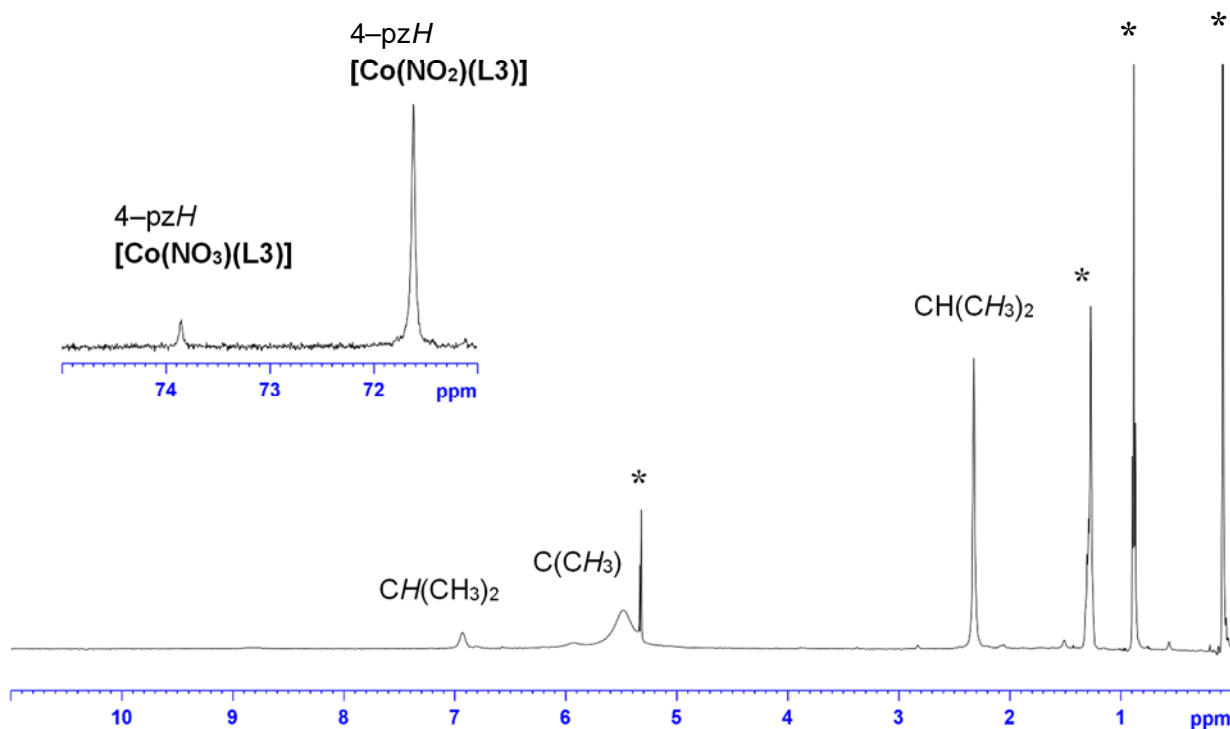


**Figure S14.**  $^1\text{H-NMR}$  spectrum of the products of the  $\text{O}_2$  reaction of  $[\text{Co}(\text{NO})(\text{L3})]$  in solution. Taken in  $\text{CD}_2\text{Cl}_2$  at room temperature (\* marks solvent, impurities, and TMS peaks).

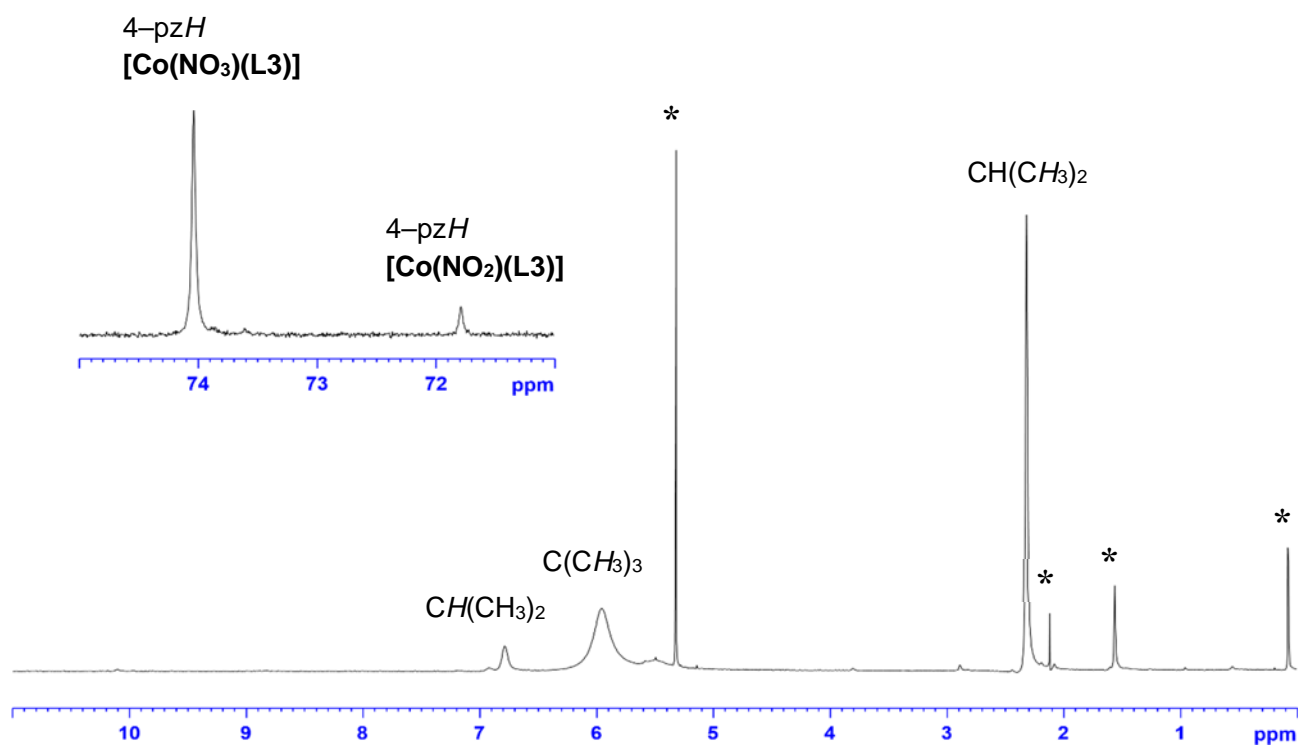


**Figure S15.**  $^1\text{H-NMR}$  spectrum of the products of the  $\text{O}_2$  reaction of  $[\text{Co}(\text{NO})(\text{L3})]$  in the solid state. Taken in  $\text{CD}_2\text{Cl}_2$  at room temperature (\* marks solvent, impurities, and TMS peaks).

**Table S2.** Molecular Orbital (MO) decompositions for [Co(NO)(L0)] ( $S = 1/2$ ), calculated with B3LYP/TZVP on the BP86/TZVP-optimized structure.

**$\alpha$ -Spin Molecular Orbitals**

MO	%Co(d)	%NO	Character <sup>a</sup>
90	76	7	$d_{xy}$
91	75	1	$d_{x^2-y^2}$
92	57	11	$d_{yz} \pi^*_h$ (bonding)
93	21	6	$d_{xz} \pi^*_v$ (bonding)
94	7	2	$\text{Pyr}(\pi) + d_{xz}$
95	8	1	$\text{Pyr}(\pi) + d_{z^2}$
96	46	11	$d_{z^2} + \pi^*_h$
97	7	1	$\text{Pyr}(\pi) + d_{xy}$
98	20	2	$\text{Pyr}(\text{N})_d d_{xy}$
99	1	0	$\text{Pyr}(\pi)$
100 (HOMO)	28	3	$\text{Pyr}(\text{N})_d d_{x^2-y^2}$
101 (LUMO)	12	77	$\pi^*_v d_{xz}$ (antibonding)
102	14	77	$\pi^*_h d_{yz}$ (antibonding)
103	2	3	$\text{Pyr}(\pi^*)$
104	2	2	$\text{Pyr}(\pi^*)$
106	0	0	$\text{Pyr}(\pi^*)$

**$\beta$ -Spin Molecular Orbitals**

MO	%Co(d)	%NO	Character <sup>a</sup>
90	38	0	$d_{x^2-y^2} \text{Pyr}(\text{N})$
91	4	1	$d_{xy} \text{Pyr}(\pi)$
92	1	1	$\text{Pyr}(\pi)$
93	0	0	$\text{Pyr}(\pi)$
94	0	1	$\text{Pyr}(\pi)$
95	0	0	$\text{Pyr}(\pi)$
96	48	38	$\pi^*_h d_{yz}$ (bonding)
97	30	60	$\pi^*_v d_{xz}$ (bonding)
98	65	3	$d_\sigma + \text{Pyr}(\text{N})$
99 (HOMO)	43	36	$d_\sigma + \pi^*_h$ (non-bonding)
100 (LUMO)	62	14	$d_{xy}/d_{xz} + \pi^*_v$ (non-bonding)
101	56	27	$d_{yz} \pi^*_h$ (antibonding)
102	55	21	$d_{xz} \pi^*_v$ (antibonding)
103	5	1	$\text{Pyr}(\pi^*) + d_{x^2-y^2}$
104	27	0	$\text{Pyr}(\pi^*) + d_{xy}$
106	0	0	$\text{Pyr}(\pi^*)$

<sup>a</sup> The nomenclature ' $a_b$ ' indicates that orbital  $a$  interacts with  $b$  and that  $a$  has a larger contribution to the resulting MO.

**Table S3.** Coordinated of the fully optimized structure of [Co(NO)(L0)], obtained with BP86/TZVP.

Co	-1.37068	-0.40828	0.36438
N	-0.56097	1.401	0.65239
N	0.76039	1.5598	0.3126
N	-0.56989	-0.44766	-1.47142
N	0.75117	-0.08906	-1.58762
N	0.26183	-1.29966	1.12994
N	1.48413	-0.82832	0.71557
C	-0.99587	2.57637	1.15134
C	0.06512	3.50368	1.13371
C	1.16437	2.83067	0.598
C	-1.00822	-0.78521	-2.70173
C	0.04986	-0.64283	-3.62168
C	1.15107	-0.20169	-2.88658
C	0.49018	-2.30706	2.0022
C	1.8791	-2.48331	2.14839
C	2.48106	-1.53174	1.32063
B	1.51438	0.34935	-0.30598
H	2.65132	0.64599	-0.56904
H	0.03701	4.53666	1.46862
H	0.01879	-0.83769	-4.68989
H	2.38885	-3.20979	2.77479
C	-2.40303	2.76319	1.62412
H	-2.64814	2.06701	2.44081
H	-2.54748	3.7879	1.99209
H	-3.1257	2.5833	0.81406
C	2.55388	3.3282	0.35247
H	2.62189	4.38563	0.64124
H	3.30055	2.76885	0.93708
H	2.83798	3.24626	-0.70777
C	3.93512	-1.26957	1.08529
H	4.21772	-0.24511	1.37179
H	4.53725	-1.96773	1.68183
H	4.20832	-1.4016	0.02729
C	-0.63889	-3.04364	2.64915
H	-0.58722	-4.12208	2.43365
H	-0.61986	-2.92273	3.74358
H	-1.59973	-2.66072	2.27635
C	-2.4168	-1.22482	-2.94898
H	-3.13274	-0.41091	-2.75732
H	-2.53674	-1.5457	-3.99253
H	-2.69473	-2.06508	-2.29517
C	2.53937	0.10682	-3.35155
H	3.28888	-0.53505	-2.86351
H	2.60816	-0.05669	-4.43538
H	2.81926	1.15179	-3.14746
N	-3.01846	-0.47759	0.4194
O	-4.18032	-0.29496	0.25275

**Table S4.** Coordinated of the fully optimized structure of [Co(NO)(L0)], obtained with M06L/TZVP.

Co	1.41956	-0.43693	-0.3433
N	0.50249	1.26491	-0.96797
N	-0.80545	1.44484	-0.63329
N	0.58314	-0.14541	1.51345
N	-0.73571	0.19864	1.54341
N	-0.23833	-1.50167	-0.88274
N	-1.45497	-0.98201	-0.55543
C	0.89289	2.35118	-1.64072
C	-0.1777	3.24236	-1.7425
C	-1.2391	2.63926	-1.09043
C	1.00103	-0.2205	2.77904
C	-0.06118	0.07642	3.63799
C	-1.14759	0.33635	2.82384
C	-0.45733	-2.66845	-1.49864
C	-1.83222	-2.90461	-1.56786
C	-2.43504	-1.81882	-0.95762
B	-1.51057	0.36096	0.21431
H	-2.64145	0.66892	0.42607
H	-0.18247	4.20407	-2.2284
H	-0.0424	0.09828	4.7149
H	-2.33055	-3.75442	-2.0039
C	2.28275	2.47888	-2.14283
H	2.55674	1.6386	-2.78248
H	2.4055	3.39365	-2.71886
H	3.00191	2.49901	-1.3219
C	-2.62401	3.12113	-0.87613
H	-2.75115	4.1077	-1.31628
H	-3.36073	2.45435	-1.32751
H	-2.86876	3.19153	0.18517
C	-3.8718	-1.53175	-0.73354
H	-4.17916	-0.60144	-1.2141
H	-4.48347	-2.33616	-1.13622
H	-4.10363	-1.43106	0.32816
C	0.67544	-3.48662	-1.99136
H	0.6263	-4.50816	-1.61323
H	0.68487	-3.54724	-3.08084
H	1.62259	-3.05058	-1.67113
C	2.40691	-0.56286	3.10388
H	3.0874	0.25054	2.84464
H	2.52113	-0.76495	4.16694
H	2.73923	-1.44232	2.55141
C	-2.53866	0.70371	3.18036
H	-3.25967	-0.03034	2.81622
H	-2.64371	0.76917	4.26106
H	-2.82572	1.66714	2.75522
N	3.08716	-0.52301	-0.23419
O	4.22965	-0.28904	-0.07763